

## Adsorption Equilibrium and Kinetics of $H_2O$ on Zeolite 13X

Young Ki Ryu\*, Seung Ju Lee, Jong Wha Kim and Chang-Ha Lee†

\*External Relations Department, Procter & Gamble Korea, Seoul 120-749, Korea

Department of Chemical Engineering, Yonsei University, Seoul 120-749, Korea

(Received 8 February 2001 • accepted 16 May 2001)

**Abstract**—The adsorption characteristics of  $H_2O$  on zeolite 13X were measured by a gravimetric method. The adsorption isotherm showed type II isotherm and was fitted by using both the excess surface work (ESW) model and Langmuir-Freundlich model. The results predicted by the Langmuir-Freundlich model were much smaller than the experimental results at higher-pressure region. However, the ESW model agreed well with the experimental data over the whole pressure region. In this case, a plot of the change in chemical potential versus the amount adsorbed gave two linear regions due to secondary effects such as capillary condensation. The experimental uptake curves were well fitted by several LDF models and solid diffusion model with the error range of 1.5-3.5%. Unlike the expectation that the more rigorous solid diffusion model would fit better, Nakao-Suzuki model showed the best agreement with experimental uptake data.

**Key words:** Excess Surface Work (ESW) Model, Water Adsorption, Zeolite 13X, Linear Driving Force (LDF), Nakao-Suzuki Model, Solid Diffusion Model

### INTRODUCTION

The need for moisture removal technology is becoming greater as product quality issues caused by moisture occur frequently. To design appropriate adsorption drying processes for moisture removal or to optimize steam regeneration processes, it is essential to select proper adsorbents and to study the adsorption rate and adsorption equilibrium.

Until now, more than 40 theories have been developed to describe adsorption equilibrium in the type II isotherm, but none of them yields a complete description of the adsorption behavior [Adolphs and Setzer, 1996]. In general, values for the specific surface area of the interface and the energetical changes in adsorption system are required to understand the adsorption behavior. In addition, the model should predict well the experimental isotherms. Usually, the lower pressure region of the adsorption branch is approximated in the type II isotherm. However, a disadvantage is that many theories hardly describe an experimental adsorption isotherm over the complete pressure range. They fail usually in the description of the upper range of the adsorption isotherms. Recently, the excess surface work (ESW) model was newly introduced to describe adsorption isotherms over the complete pressure range [Adolphs and Setzer, 1996]. The new model describes adsorption isotherms with a two-parameter function. It was shown that the model was successfully extended to adsorption isotherms of porous solid materials and finely dispersed powders [Adolphs and Setzer, 1998].

To properly design an adsorber, information of the adsorption kinetics is also needed beside the adsorption equilibria. The reason for this is simply that most practical adsorbents used in industries are porous and the overall adsorption rate is limited by the ability of adsorbate molecules to diffuse into the adsorbent pore.

The linear driving force (LDF) model, which was originally proposed by Gleuckauf and Coates for adsorption chromatography, is frequently used for describing adsorption kinetics because it is simple, analytical, and physically consistent [Sircar et al., 2000]. In the LDF model, the overall mass transfer coefficient is the only rate parameter, which is usually related to the intraparticle diffusion coefficient. The model assumes that the adsorbent particle temperature is uniform at all times. Also, for a step-function change in concentration, the solution of mass balance equation for a particle was approximated by Vermeulen [Yang, 1987]. Moreover, Nakao and Suzuki have examined the accuracy of LDF equation as applied to the Skarstrom cycle. The analysis of the coefficient (K) in this study was made for a single particle and was extended to adsorbents [Suzuki, 1990]. By comparing LDF model with the more rigorous solid diffusion model, Sircar and Hufton [Sircar et al., 2000] recently demonstrated the reason why the LDF model worked well in practice.

The choice of adsorbent depends mainly on the nature of the gas stream and the level of dehydration required. Zeolite 13X is one of the adsorbents that are frequently used for drying processes [Yang, 1987]. In this work, the studies for adsorption equilibrium and kinetics of  $H_2O$  on zeolite 13X were conducted. The adsorption equilibria were measured by a gravimetric method to the pressure region that capillary condensation took place. The adsorption isotherms were fitted by both excess surface work model and existing Langmuir-Freundlich model to verify their effectiveness. Also, the kinetic data were compared with several LDF-type models and solid diffusion model.

### MODELS FOR ADSORPTION ISOTHERMS

#### 1. Excess Surface Work Model

An adsorption system where particles are adsorbed on a solid surface or on another phase will be assumed to be an open system

\*To whom correspondence should be addressed.  
E-mail: leech@mail.yonsei.ac.kr

in mechanical and thermal equilibrium. The temperature  $T$  and the chemical potential  $\mu$  are equal both in the gas (or liquid) phase and the adsorbed phase of an adsorption system.

$$\mu = \mu_{gas} = \mu_{ads} \text{ and } T = T_{gas} = T_{ads} \quad (1)$$

The change of the chemical potential is presented by the ratio of the pressure ( $p$ ) to saturation vapor pressure ( $p_s$ ) at the absolute temperature ( $T$ ).

$$\Delta\mu = RT \ln(p/p_s) \quad (2)$$

For further purposes, excess surface work (ESW) is defined as the product of the amount adsorbed ( $n_{ads}$ ) and the change in the chemical potential ( $\Delta\mu$ ). The ESW was proved useful in examining adsorption isotherms [Adolphs and Setzer, 1996].

$$\Phi = n_{ads} \cdot \Delta\mu \quad (3)$$

It is evident that the ESW must be negative in adsorption processes when the adsorbed amount is defined as positive. No further changes occur when the saturation vapor pressure  $p_s$  is reached. The ESW becomes zero at zero coverage and at infinite coverage when the change in the chemical potential diminishes. It is obvious that the ESW must be a function with a minimum. The pressure and the adsorbed amount can be determined experimentally. Therefore, the ESW can be easily calculated. The basic idea for an adsorption process is that the ESW will minimize at the biggest adsorbate-adsorbate and adsorbate-adsorbent interaction, which is defined as the monolayer capacity. This yields a differential equation at the point  $n_{ads} = n_{mono}$ .

$$d\Phi = \Delta\mu \, dn_{ads} + n_{ads} \, d(\Delta\mu) = 0 \quad (4)$$

By integration and linearization, the following equation is obtained.

$$\ln|\Delta\mu| = -\frac{1}{n_{mono}} n_{ads} + \ln|\Delta\mu_0| \quad (5)$$

The variable  $\Delta\mu_0$  is the initial change in chemical potential where adsorption starts, as related to saturation under isothermal conditions. A plot of  $\ln|\Delta\mu|$  against  $n_{ads}$  gives the monolayer amount ( $n_{mono}$ ) from the reciprocal slope and the initial potential ( $\Delta\mu_0$ ) from the ordinate intercept. With the results of the new model, it is possible to calculate recursively an adsorption isotherm by the following equation.

$$n_{ads} = -n_{mono} \ln \left| \frac{\Delta\mu}{\Delta\mu_0} \right| \quad (6)$$

## 2. Langmuir-Freundlich Model

Because of the limited success of the Langmuir model in predicting equilibria, several authors have modified the equation by the introduction of a power law expression of Freundlich [Ruthven, 1984].

$$\frac{q}{q_m} = \frac{bp^n}{1+bp^n} \quad (7)$$

Although not thermodynamically consistent, it has been shown that this expression provided a reasonably good empirical correlation of equilibrium data for a number of simple gases on adsorbents and is widely used for design purposes.

## MODELS FOR ADSORPTION KINETICS

### 1. Solid Diffusion Model

When effective diffusivity is constant, intraparticle diffusion rate can be expressed by the following equation.

$$\frac{\partial q}{\partial t} = \frac{D_e}{r^2} \frac{\partial}{\partial r} \left( r^2 \frac{\partial q}{\partial r} \right) \quad (8)$$

The following analytical solution can be obtained for the initial and boundary conditions [Ruthven, 1984].

$$\frac{m_t}{m_e} = 1 - \frac{6}{\pi^2} \sum_{n=1}^{\infty} \frac{1}{n^2} \exp\left(-\frac{n^2 \pi^2 D_e t}{r_p^2}\right) \quad (9)$$

### 2. Linear Driving Force (LDF) Model

LDF equation approximates the rate of sorption by a spherical particle that is subject to varying increases in the ambient fluid concentration (an exponentially increasing concentration and a linearly increasing concentration) [Yang, 1987]. The approximation, as given by Glueckauf and Coates, is

$$\frac{\partial \bar{q}}{\partial t} = \frac{15 D_e}{R_p^2} (q^* - \bar{q}) \quad (10)$$

### 3. Vermeulen Model

For a step function change in concentration, the solution for the mass transfer into an adsorbent was approximated by Vermeulen as the following.

$$\frac{\partial \bar{q}}{\partial t} = \frac{\pi D_e}{R_p^2} \left( \frac{q^2 - \bar{q}^2}{2\bar{q}} \right) \quad (11)$$

The boundary condition of a single step change in bulk concentration is a good representation of the condition in an adsorber bed when the adsorption isotherm is very steep, that is, when the Langmuir constant approaches an irreversible isotherm. Therefore, this equation is superior to the LDF equation for a steep isotherm [Yang, 1987].

### 4. Nakao & Suzuki Model

The applicability of the LDF approximation to the pressure swing adsorption (PSA) process has been discussed by Nakao and Suzuki [Suzuki, 1990; Yang, 1987]. In an idealized two-step cycle, the amount adsorbed in the particle at steady state is calculated by solving the mass balance equation with the LDF approximation. The LDF model with a coefficient of 15 in Eq. (9) underestimates the rate of uptake when the amount adsorbed is too small, which is the case when the half-cycle time ( $=D_e t / R_p^2$ ) is small. Therefore, they pointed out that the value of the coefficient  $K$  in the LDF approximation is given as a function of the half-cycle time.

$$\frac{\partial \bar{q}}{\partial t} = \frac{KD_e}{R_p^2} (q^* - \bar{q}) \quad (12)$$

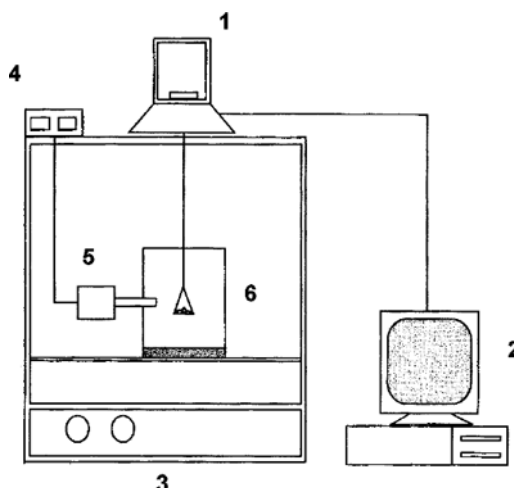
In the case of adsorption kinetics in adsorbents, partial differential equations were decomposed into ordinary differential equations and then solved by IVPAG routine of IMSL library [IMSL, 1989]. The 4<sup>th</sup> order Runge-Kutta method was used for LDF, Nakao-Suzuki and Vermeulen models.

## EXPERIMENTAL

### 1. Adsorbents

**Table 1. Characteristics of zeolite 13X**

Characteristics	Values
Type	Bead
Normal pellet size [mesh]	4-8
Average pellet size, $R_p$ [cm]	0.11
Pellet density [g/cm <sup>3</sup> ]	1.1
Heat capacity [cal/g·K]	0.22
Particle porosity [-]	0.23
Bulk density [lb/ft <sup>3</sup> ]	43
Maximum heat of adsorption [BTU/lb]	1800

**Fig. 1. Apparatus of adsorption of H<sub>2</sub>O on zeolite 13X.**

- |                 |              |
|-----------------|--------------|
| 1. Microbalance | 4. Indicator |
| 2. Computer     | 5. Sensor    |
| 3. Oven         | 6. Beaker    |

The adsorbent used in this study was pelletized zeolite 13X, which had a bi-dispersed pore structure with micropores and macropores. Prior to each experiment, the adsorbent had been activated for over 7 hours in the furnace at 340 °C. The characteristics of the adsorbent are listed in Table 1.

## 2. Experimental Apparatus

Fig. 1 shows a schematic diagram of experimental apparatus. The gravimetric method was used to investigate adsorption characteristics of water vapor on zeolite 13X. The hangdown basket from a precise balance (HR-300, AND Co.) was equipped on the oven to keep a constant temperature. When the temperature and humidity sensor (HMP111Y, Vaisala Co.) equipped in the beaker displayed constant values, the activated adsorbents were put in the mesh basket. Desired values of relative humidity were obtained by adding several kinds of salts into beaker filled with distilled deionized water. In order to monitor a constant experimental condition, the values of humidity and temperature were displayed through an indicator. The adsorbed amounts vs. time were automatically recorded through interface with a computer. The experimental ranges of temperature and relative humidity were 298-318 K and 15-90%, respectively.

## RESULTS AND DISCUSSION

### 1. Adsorption Equilibrium

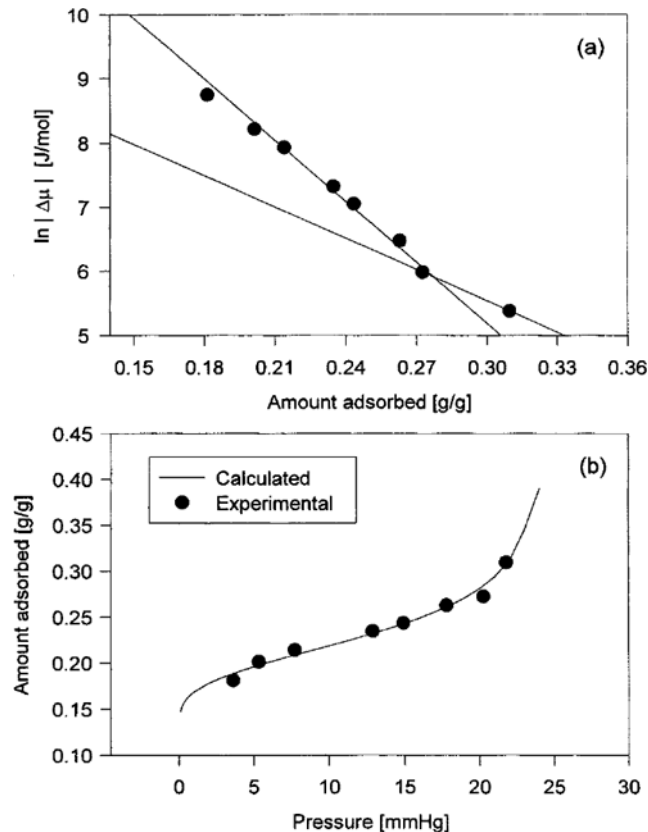


**Fig. 2. Adsorption isotherm of water at 298 K on zeolite 13X.**  
(a) linearized form of water adsorption, (b) recursively calculated isotherms by ESW model

By plotting  $\ln|\Delta\mu|$  against  $n_{\text{ads}}$ , the monolayer amount ( $n_{\text{mono}}$ ) and the initial potential ( $\Delta\mu_0$ ) could be obtained from the reciprocal slope and from the ordinate intercept, respectively. The integral plot of water adsorption versus the change of chemical potential showed two linear regions described by two pairs of parameters as shown in Figs. 2(a), 3(a), and 4(a). Regardless of operating temperature, the transition point was placed on the range of 0.26-0.28 g/g of amounts adsorbed. One pair of parameters described the lower pressure region, whereas the other pair described the higher pressure region. In the lower pressure region considering pure physical adsorption, the monolayer adsorption capacity could be calculated by the following equation [Adolfs and Setzer, 1998].

$$\ln|\Delta\mu| = -\frac{1}{n_{\text{mono}}} n_{\text{ads}} + \ln|\Delta\mu_0| \quad (13a)$$

Also, the other linear line in the higher pressure region was made of second and more effects such as transition to capillary condensation

$$\ln|\Delta\mu| = -\frac{1}{n_2} n_{\text{ads}} + \ln|\Delta\mu_2| \quad (13b)$$

where  $n_2$  is the amount adsorbed when excess surface work is minimized due to secondary effects. The calculated two pairs of parameters by Eqs. (13a) and (13b) using plot of  $\ln|\Delta\mu|$  against  $n_{\text{ads}}$  are listed on Table 2. As can be seen, the monolayer capacity was slightly decreased with temperature in the experimental range.

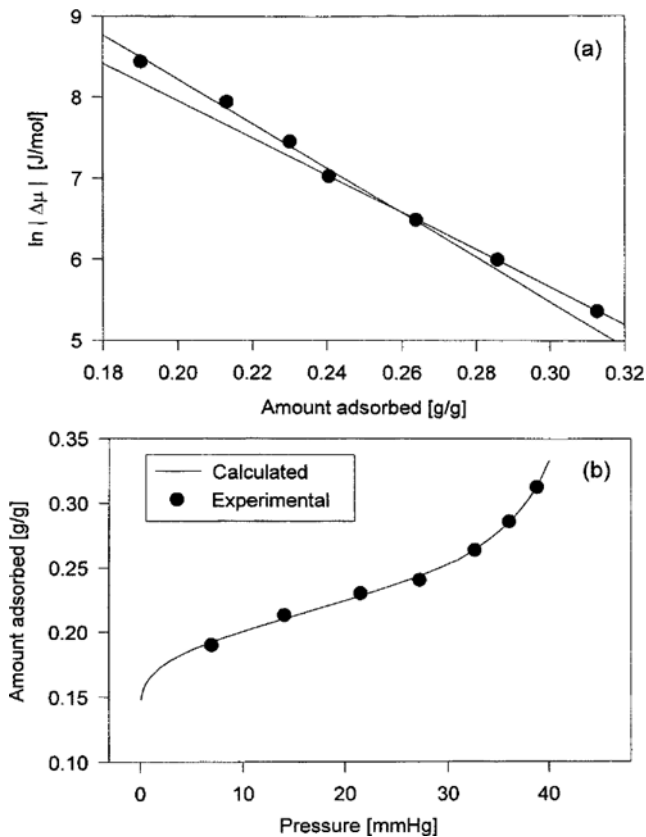


**Fig. 3. Adsorption isotherm of water at 308 K on zeolite 13X.**  
(a) linearized form of water adsorption, (b) recursively calculated isotherms by ESW model

As shown in Figs. 2(b), 3(b), and 4(b), adsorption isotherms were recursively calculated by using Eq. (6) with two pairs of parameters obtained from Eqs. (13a) and (13b). The calculated isotherm has well fitted experimental data even for the higher pressure region that capillary condensation occurred. The averaged error values for 298 K, 308 K and 318 K were 1.1%, 0.7% and 1.6%, respectively. The pressure that capillary condensation occurred was increased as the temperature increased.

Fig. 5 shows comparison of the calculated isotherms between the Langmuir-Freundlich model and the ESW model. The Langmuir-Freundlich model could not predict experimental data in capillary condensation region. The model gave too small values of the amount adsorbed at higher pressure, whereas the ESW model showed good agreement with experimental data over whole pressure region. Moreover, BET equation was not able to properly predict experimental data because the pressure range of validity of the BET equation was  $p/p_0 = 0.05-0.3$ . For a relative pressure above 0.3, there exists capillary condensation, which is not amenable to multilayer analysis [Do, 1998].

Also, the adsorption equilibrium at low pressure region in  $\text{H}_2\text{O}$ /zeolite 13X system showed near irreversible isotherm type. It implies that the high energy is needed to regenerate the adsorbent. The capillary condensation pressure increased with the increase of the system temperature. This notes that the capillary condensation pressure strongly depends on the system temperature such as the saturated pressure.

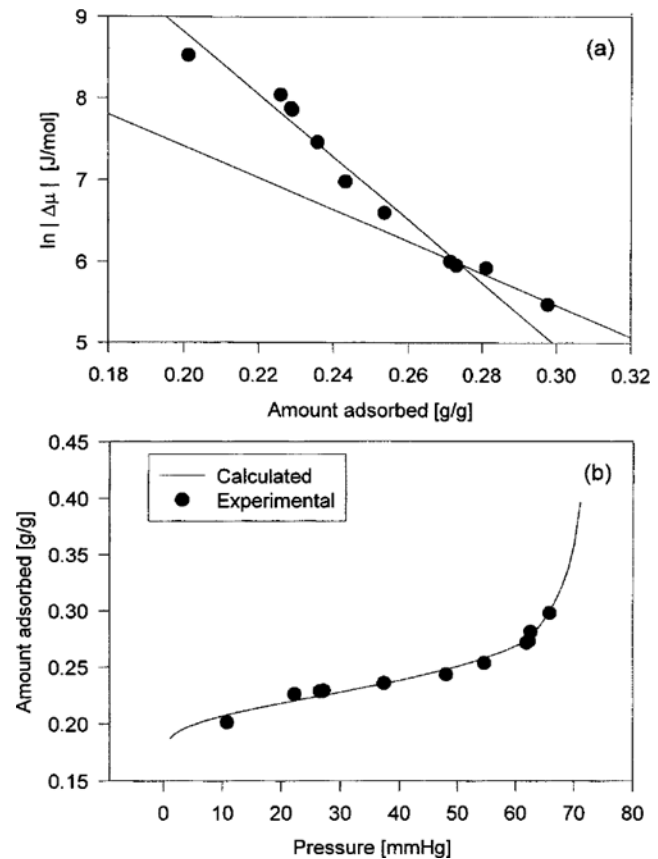


**Fig. 4. Adsorption isotherm of water at 318 K on zeolite 13X.**  
(a) linearized form of water adsorption, (b) recursively calculated isotherms by ESW model

**Table 2. The values of calculated parameters**

Parameter	Temperature		
	298 K	308 K	318 K
$\ln \Delta\mu_1 $	13.3	13.7	16.5
$n_{\text{mono}}$	0.0386	0.0364	0.0259
$\ln \Delta\mu_2 $	10.4	12.5	11.3
$n_2$	0.0614	0.0435	0.0512

## 2. Adsorption Rate

The adsorption rate was presented at a relative humidity (RH) condition in order to compare clearly the results among the several experimental results. Fig. 6 shows characteristics of uptake curves for water vapor adsorption. At early stage of adsorption, uptake curves for higher relative humidity show faster adsorption. This is because effective diffusivity is bigger at higher relative humidity until it reaches a certain relative humidity where capillary condensation or micropore filling occurs, as shown in Fig. 7. In the case of 93% RH, the uptake curve also shows very fast adsorption at an early stage. However, the decreased effective diffusivity caused by capillary condensation or micropore filling resulted in longer time to reach at adsorption equilibrium.

Fig. 7 shows values of effective diffusivities that were obtained by applying solid diffusion model for each relative humidity. The effective diffusivity increased with an increase in relative humidity

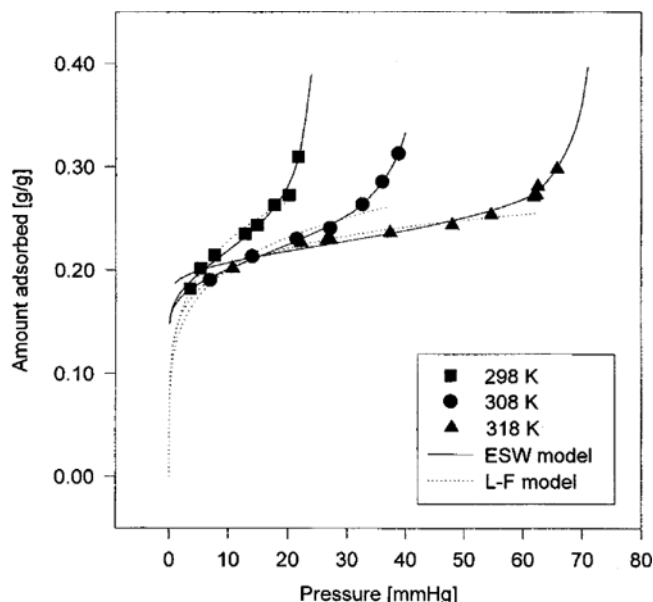


Fig. 5. Recursively calculated isotherms of water by ESW model and L-F model at 298 K, 308 K and 318 K, respectively.

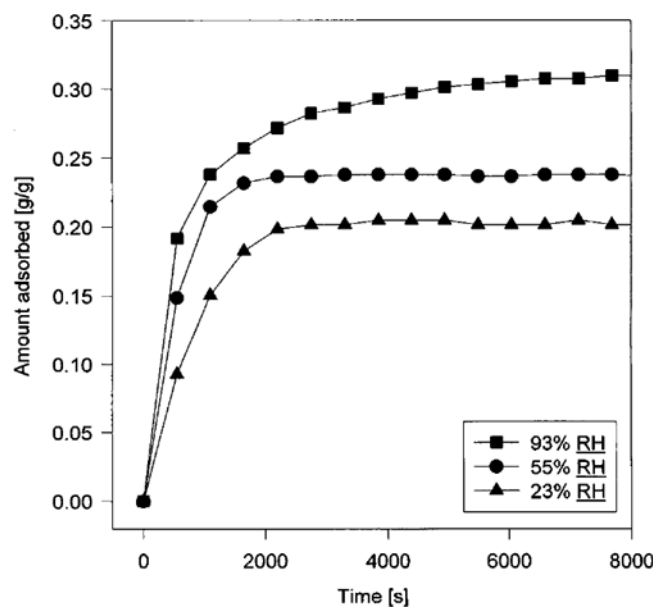


Fig. 6. Uptake curves of water at 398.15 K in 23%, 55%, and 93% RH, respectively.

and then decreased at around 80%RH. This decrease may be due to multilayer adsorption, capillary condensation or micropore filling that occurs at high humidity region. Also, the effective diffusivities showed higher values at higher temperature, because the motions of adsorptive molecules become more active with an increase in temperature. However, the temperature effect on effective diffusivity became smaller at the high humidity region in which capillary condensation occurred.

The calculated uptake curves by solid diffusion, LDF, Vermeulen, and Nakao-Suzuki models are shown in Fig. 8. It is reported that Vermeulen model is more suitable for Langmuir type isotherm or irreversible isotherm that show strongly favorable adsorption behav-

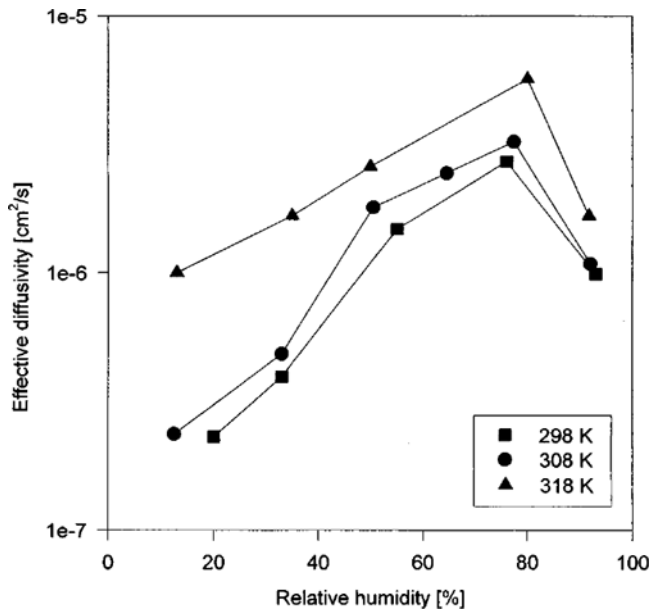


Fig. 7. Effective diffusivity calculated by solid diffusion model.

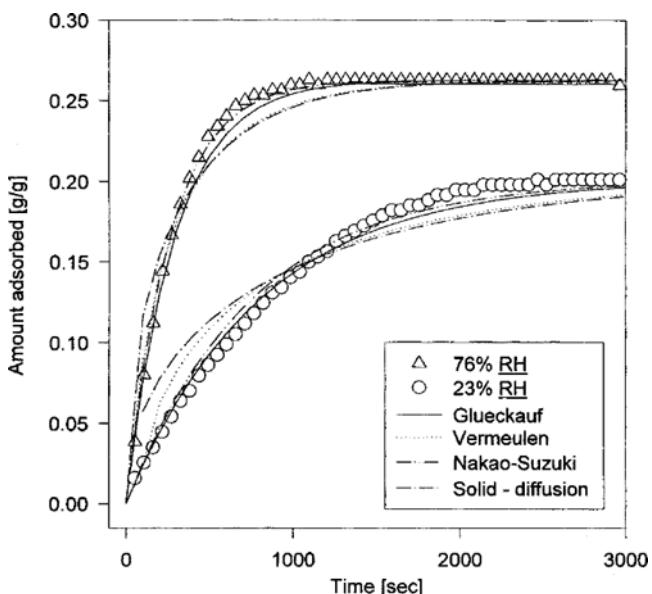


Fig. 8. Uptake curves of water at 298 K in 76% and 23% RH.

ior at early stage [Yang, 1987]. Like this, the Vermeulen model predicted well the experimental data at early stage of adsorption in the high humid condition. Meanwhile, this model in the low RH condition overestimated experimental data at early stage of adsorption. Also, the LDF with a coefficient of 15 [Yang, 1987] underestimates the rate of uptake when the amount adsorbed is small. In the case of Nakao-Suzuki LDF model, the constants K at 298 K were 16.8 and 16 for 76%RH and 23%RH, respectively, and those values were bigger than that of the Glueckauf model (K=15). The Nakao-Suzuki model provided better fit for water adsorption on zeolite 13X than the more rigorous solid diffusion model and other models. The errors averaged over 3000 seconds were 1.5%, 1.1%, 3.6% and 3.2% for LDF, Nakao-Suzuki, solid diffusion and Vermeulen models, respectively. There is a substantial difference in the characteristics of iso-

thermal uptake curves on adsorbent particles by the LDF and the solid diffusion model. Although the solid diffusion model of gas transport in adsorbent particles provides a more realistic mechanism, the model is not adequate for describing exterior mass transfer and intraparticle transport phenomena. Kim et al. [Kim et al., 1995] showed that the results of all five steps in PSA were successfully predicted by the LDF model considering an energy balance and nonlinear isotherm. Recently, Sircar et al. [Sircar and Hutton, 2000] demonstrated the LDF model could be used as a practical tool for describing the adsorption kinetics on heterogeneous solids. The results of this study also show that the LDF model is adequately used to describe the adsorption kinetics as long as detailed equations for mass transfer resistance are not incorporated into the solid diffusion model.

## CONCLUSIONS

The adsorption of water vapor on zeolite 13X showed type II isotherm of Brunauer's classification. The Langmuir-Freundlich model gives too small values of the amount adsorbed at higher pressure. However, the ESW model could be successfully applied for the description of water adsorption isotherms on zeolite 13X over the whole pressure region. In this case, a plot of the absolute value of the change in chemical potential versus the amount adsorbed gave two linear regions due to secondary effects such as capillary condensation.

The effective diffusivity was increased with an increase in relative humidity, but it began to decrease near the capillary condensation region. The experimental uptake curves were well fitted by solid diffusion, LDF, Vennemen and Nakao-Suzuki models with the error range of 1.5-3.5%. Although it was expected that the more rigorous solid diffusion model would fit better than other models, the Nakao-Suzuki model showed the best agreement with experimental data.

## NOMENCLATURE

$D_e$	: effective diffusivity [ $\text{cm}^2/\text{sec}$ ]
$K$	: Henry constant [ $\text{mmol/g} \cdot \text{atm}$ ]
$m_t$	: mass adsorbed at time $t$ [g]
$m_\infty$	: mass adsorbed at $t \rightarrow \infty$ [g]
$n_{ads}$	: the amount adsorbed [mol/g]
$n_{mono}$	: the monolayer capacity [mol/g]
$p$	: pressure [mmHg]
$p_s$	: saturation vapor pressure [mmHg]

$\bar{q}$	: amount adsorbed (adsorbed phase concentration) [g/g]
$\bar{q}_\infty$	: value of $q$ averaged over a crystal or pellet volume [g/g]
$q^*$	: the amount adsorbed in equilibrium with the bulk flow concentration [g/g]
$r$	: radial distance in crystal [cm]
$r_p$	: micropore radius [cm]
$R$	: the gas constant [=8.314 J/mol·K]
$R_p$	: pellet radius [cm]
$t$	: time [sec]
$T$	: temperature [K]

## Greek Letters

$\Phi$	: excess surface work [J/g]
$\Delta\mu$	: the change in the chemical potential [J/mol]
$\Delta\mu_0$	: the initial change in chemical potential where adsorption starts [J/mol]

## REFERENCES

- Adolphs, J. and Setzer, M. J., "A Model to Describe Adsorption Isotherms," *J. Colloid and Interface Sci.*, **180**, 70 (1996).
- Adolphs, J. and Setzer, M. J., "Energetic Classification of Adsorption Isotherms," *J. Colloid and Interface Sci.*, **184**, 443 (1996).
- Adolphs, J. and Setzer, M. J., "Description of Gas Adsorption on Porous and Dispersed Systems with the Excess Surface Work Model," *J. Colloid and Interface Sci.*, **207**, 349 (1998).
- Do, D. D., "Adsorption Analysis: Equilibria and Kinetics," Imperial College Press, London (1998).
- IMSL MATH/LIBRARY, "FORTRAN Subroutine for Mathematical Application Ver. 1.1 User's Manual," IMSL Inc. (1989).
- Kaiger, J. and Ruthven, D. M., "Diffusion in Zeolite and other Microporous Solids," John Wiley & Sons, Inc., New York (1992).
- Kim, W. G., Yang, J., Han, S., Cho, C., Lee, C. H. and Lee, H. J., "Experimental and Theoretical Study on  $\text{H}_2/\text{CO}_2$  Separation by a Five-Step One-Column PSA Process," *Korean J. Chem. Eng.*, **12**, 5 (1995).
- Ruthven, D. M., Farooq, S. and Knabel, K. S., "Pressure Swing Adsorption," VCH Publishers, Inc., New York (1994).
- Ruthven, D. M., "Principles of Adsorption and Adsorption Processes," John Wiley & Sons, Inc., New York (1984).
- Sircar, S. and Hutton, J. R., "Why Does the Linear Driving Force Model for Adsorption Kinetics Work," *Adsorption*, **6**, 137 (2000).
- Suzuki, M., "Adsorption Engineering," Kodansha Ltd, Tokyo (1990).
- Yang, R. T., "Gas Separation by Adsorption Processes," Butterworths, Boston (1987).